SUPPLEMENTARY of "Toward Consistent and Efficient Map-based Visual-inertial Localization: Theory Framework and Filter Design"

***Abstract*—This document provides the theoretical proofs mentioned in the main paper "Toward Consistent and Efficient Map-based Visual-inertial Localization: Theory Framework and Filter Design". Besides, some additional experimental results and corresponding analyses are given. All the notations, equation numbers, reference numbers and section numbers are identical to those in the main paper.**

APPENDIX A
DERIVATION OF ERROR PROPAGATION FUNCTION

From (8) and (12), we need to derive the linearized error kinematics:

$$\frac{d}{dt}\mathbf{e}_t = \left(\frac{d}{dt}\boldsymbol{\eta}_{A_t}, \frac{d}{dt}\boldsymbol{\xi}_{B_t}\right). \tag{100}$$

To derive $\frac{d}{dt}\boldsymbol{\eta}_{A_t}$, recall the definition of the *right invariant error* (11), we have:

$$\begin{aligned}
\frac{d}{dt}({}^L\hat{\mathbf{R}}_{I_t}{}^L\mathbf{R}_{I_t}^{-1}) =& {}^L\hat{\mathbf{R}}_{I_t}(\boldsymbol{\omega}_t - \hat{\mathbf{b}}_{g_t})_\times {}^L\mathbf{R}_{I_t}^\top \\
&+ {}^L\hat{\mathbf{R}}_{I_t}({}^L\mathbf{R}_{I_t}(\boldsymbol{\omega}_t - \mathbf{b}_{g_t} - \mathbf{w}_{g_t})_\times)^\top \\
\frac{d}{dt}({}^L\hat{\mathbf{R}}_{I_t}{}^L\mathbf{R}_{I_t}^{-1}) =& {}^L\hat{\mathbf{R}}_{I_t}(\boldsymbol{\omega}_t - \hat{\mathbf{b}}_{g_t})_\times {}^L\hat{\mathbf{R}}_{I_t}^\top\boldsymbol{\eta}_R \\
&- {}^L\hat{\mathbf{R}}_{I_t}(\boldsymbol{\omega}_t - \mathbf{b}_{g_t} - \mathbf{w}_{g_t})_\times {}^L\hat{\mathbf{R}}_{I_t}^\top\boldsymbol{\eta}_R \\
\frac{d}{dt}({}^L\hat{\mathbf{R}}_{I_t}{}^L\mathbf{R}_{I_t}^{-1}) =& {}^L\hat{\mathbf{R}}_{I_t}(-\boldsymbol{\xi}_{B_{gt}} + \mathbf{w}_{g_t})_\times {}^L\hat{\mathbf{R}}_{I_t}^\top\boldsymbol{\eta}_R \\
\frac{d}{dt}({}^L\hat{\mathbf{R}}_{I_t}{}^L\mathbf{R}_{I_t}^{-1}) =& ({}^L\hat{\mathbf{R}}_{I_t}(-\boldsymbol{\xi}_{B_{gt}} + \mathbf{w}_{g_t}))_\times\boldsymbol{\eta}_R \\
\frac{d}{dt}(\mathbf{I} + (\boldsymbol{\xi}_{\boldsymbol{\theta}_{LI_t}})_\times) \approx& ({}^L\hat{\mathbf{R}}_{I_t}(-\boldsymbol{\xi}_{B_{gt}} + \mathbf{w}_{g_t}))_\times(\mathbf{I} + (\boldsymbol{\xi}_{\boldsymbol{\theta}_{LI_t}})_\times) \\
\frac{d}{dt}((\boldsymbol{\xi}_{\boldsymbol{\theta}_{LI_t}})_\times) \approx& ({}^L\hat{\mathbf{R}}_{I_t}(-\boldsymbol{\xi}_{B_{gt}} + \mathbf{w}_{g_t}))_\times \\
\frac{d}{dt}\boldsymbol{\xi}_{\boldsymbol{\theta}_{LI_t}} \approx& {}^L\hat{\mathbf{R}}_{I_t}(-\boldsymbol{\xi}_{B_{gt}} + \mathbf{w}_{g_t}).
\end{aligned} \tag{101}$$

$$\begin{aligned}
\frac{d}{dt}({}^L\hat{\mathbf{v}}_{I_t} - {}^L\hat{\mathbf{R}}_{I_t}{}^L\mathbf{R}_{I_t}^{-1}{}^L\mathbf{v}_{I_t}) =& {}^L\hat{\mathbf{R}}_{I_t}(\mathbf{a}_t - \hat{\mathbf{b}}_{a_t}) + \mathbf{g} - \\
&\left(\frac{d}{dt}({}^L\hat{\mathbf{R}}_{I_t}{}^L\mathbf{R}_{I_t}^{-1}){}^L\mathbf{v}_{I_t} + \right. \\
&\left. {}^L\hat{\mathbf{R}}_{I_t}{}^L\mathbf{R}_{I_t}^{-1}({}^L\mathbf{R}_{I_t}(\mathbf{a}_t - \mathbf{b}_{a_t} - \mathbf{w}_{a_t}) + \mathbf{g})\right) \\
\frac{d}{dt}(\boldsymbol{\xi}_{\mathbf{v}_{LI_t}}) =& {}^L\hat{\mathbf{R}}_{I_t}(\mathbf{a}_t - \hat{\mathbf{b}}_{a_t}) + \mathbf{g} - ({}^L\hat{\mathbf{R}}_{I_t}(-\boldsymbol{\xi}_{B_{gt}} + \mathbf{w}_{g_t}))_\times \\
&\boldsymbol{\eta}_R{}^L\mathbf{v}_{I_t} - {}^L\hat{\mathbf{R}}_{I_t}(\mathbf{a}_t - \mathbf{b}_{a_t} - \mathbf{w}_{a_t}) - \boldsymbol{\eta}_R\mathbf{g} \\
\frac{d}{dt}(\boldsymbol{\xi}_{\mathbf{v}_{LI_t}}) =& {}^L\hat{\mathbf{R}}_{I_t}(-\boldsymbol{\xi}_{B_{at}} + \mathbf{w}_{a_t}) + \mathbf{g} - \boldsymbol{\eta}_R\mathbf{g} - \\
&({}^L\hat{\mathbf{R}}_{I_t}(-\boldsymbol{\xi}_{B_{gt}} + \mathbf{w}_{g_t}))_\times({}^L\hat{\mathbf{v}}_{I_t} - \boldsymbol{\xi}_{\mathbf{v}_{LI_t}}) \\
\frac{d}{dt}(\boldsymbol{\xi}_{\mathbf{v}_{LI_t}}) \approx& {}^L\hat{\mathbf{R}}_{I_t}(-\boldsymbol{\xi}_{B_{at}} + \mathbf{w}_{a_t}) + \mathbf{g} - (\mathbf{I} + (\boldsymbol{\xi}_{\boldsymbol{\theta}_{LI_t}})_\times)\mathbf{g} - \\
&({}^L\hat{\mathbf{R}}_{I_t}(-\boldsymbol{\xi}_{B_{gt}} + \mathbf{w}_{g_t}))_\times({}^L\hat{\mathbf{v}}_{I_t} - \boldsymbol{\xi}_{\mathbf{v}_{LI_t}}) \\
\frac{d}{dt}(\boldsymbol{\xi}_{\mathbf{v}_{LI_t}}) \approx& {}^L\hat{\mathbf{R}}_{I_t}(-\boldsymbol{\xi}_{B_{at}} + \mathbf{w}_{a_t}) + (\mathbf{g})_\times\boldsymbol{\xi}_{\boldsymbol{\theta}_{LI_t}} + \\
&({}^L\hat{\mathbf{v}}_{I_t})_\times {}^L\hat{\mathbf{R}}_{I_t}(-\boldsymbol{\xi}_{B_{gt}} + \mathbf{w}_{g_t}).
\end{aligned} \tag{102}$$

Analogously,

$$\begin{aligned}
&\frac{d}{dt}({}^L\hat{\mathbf{p}}_{I_t} - {}^L\hat{\mathbf{R}}_{I_t}{}^L\mathbf{R}_{I_t}^{-1}{}^L\mathbf{p}_{I_t}) = {}^L\hat{\mathbf{v}}_{I_t} - \\
&\left(\frac{d}{dt}({}^L\hat{\mathbf{R}}_{I_t}{}^L\mathbf{R}_{I_t}^{-1}){}^L\mathbf{p}_{I_t} + {}^L\hat{\mathbf{R}}_{I_t}{}^L\mathbf{R}_{I_t}^{-1}{}^L\mathbf{v}_{I_t}\right) \\
&\frac{d}{dt}(\boldsymbol{\xi}_{\mathbf{p}_{LI_t}}) \approx \boldsymbol{\xi}_{\mathbf{v}_{LI_t}} + ({}^L\hat{\mathbf{p}}_{I_t})_\times({}^L\hat{\mathbf{R}}_{I_t}(-\boldsymbol{\xi}_{B_{gt}} + \mathbf{w}_{g_t})).
\end{aligned} \tag{103}$$

$$\begin{aligned}
&\frac{d}{dt}({}^L\hat{\mathbf{p}}_{f_t} - {}^L\hat{\mathbf{R}}_{I_t}{}^L\mathbf{R}_{I_t}^{-1}{}^L\mathbf{p}_{f_t}) = -\frac{d}{dt}({}^L\hat{\mathbf{R}}_{I_t}{}^L\mathbf{R}_{I_t}^{-1}){}^L\mathbf{p}_{f_t} \\
&\frac{d}{dt}(\boldsymbol{\xi}_{\mathbf{p}_{Lf_t}}) \approx ({}^L\hat{\mathbf{p}}_{f_t})_\times({}^L\hat{\mathbf{R}}_{I_t}(-\boldsymbol{\xi}_{B_{gt}} + \mathbf{w}_{g_t}))
\end{aligned} \tag{104}$$

$$\begin{aligned}
&\frac{d}{dt}({}^L\hat{\mathbf{p}}_{G_t} - {}^L\hat{\mathbf{R}}_{I_t}{}^L\mathbf{R}_{I_t}^{-1}{}^L\mathbf{p}_{G_t}) = -\frac{d}{dt}({}^L\hat{\mathbf{R}}_{I_t}{}^L\mathbf{R}_{I_t}^{-1}){}^L\mathbf{p}_{G_t} \\
&\frac{d}{dt}(\boldsymbol{\xi}_{\mathbf{p}_{LG_t}}) \approx ({}^L\hat{\mathbf{p}}_{G_t})_\times({}^L\hat{\mathbf{R}}_{I_t}(-\boldsymbol{\xi}_{B_{gt}} + \mathbf{w}_{g_t}))
\end{aligned} \tag{105}$$

So, the linearized error kinematics of be written as (13).

APPENDIX B
DERIVATION OF THE JACOBIAN MATRIX OF THE OBSERVATION FUNCTION

To derive the Jacobian matrix of (19), we have

$$\begin{aligned}
&h({}^L\mathbf{R}_{I_t}^\top({}^L\mathbf{p}_{f_t} - {}^L\mathbf{p}_{I_t})) - h({}^L\hat{\mathbf{R}}_{I_t}^\top({}^L\hat{\mathbf{p}}_{f_t} - {}^L\hat{\mathbf{p}}_{I_t})) \\
&\approx \nabla h|_{\hat{\mathfrak{q}}}(\mathfrak{q} - \hat{\mathfrak{q}}) \\
&= \nabla h|_{\hat{\mathfrak{q}}}\left[{}^L\mathbf{R}_{I_t}^\top({}^L\mathbf{p}_{f_t} - {}^L\mathbf{p}_{I_t}) - {}^L\hat{\mathbf{R}}_{I_t}^\top({}^L\hat{\mathbf{p}}_{f_t} - {}^L\hat{\mathbf{p}}_{I_t})\right] \\
&= \nabla h|_{\hat{\mathfrak{q}}}\left[{}^L\hat{\mathbf{R}}_{I_t}^\top\left[{}^L\hat{\mathbf{R}}_{I_t}{}^L\mathbf{R}_{I_t}^\top({}^L\mathbf{p}_{f_t} - {}^L\mathbf{p}_{I_t}) - ({}^L\hat{\mathbf{p}}_{f_t} - {}^L\hat{\mathbf{p}}_{I_t})\right]\right] \\
&= \nabla h|_{\hat{\mathfrak{q}}}\left[{}^L\hat{\mathbf{R}}_{I_t}^\top\left(\boldsymbol{\xi}_{\mathbf{p}_{LI_t}} - \boldsymbol{\xi}_{\mathbf{p}_{Lf_t}}\right)\right] \\
&= \nabla h|_{\hat{\mathfrak{q}}}{}^L\hat{\mathbf{R}}_{I_t}^\top\begin{bmatrix}\mathbf{0}_3 & \mathbf{0}_3 & \mathbf{I}_3 & -\mathbf{I}_3 & \mathbf{0}_3 & \mathbf{0}_3 & \mathbf{0}_3 & \mathbf{0}_3\end{bmatrix}\boldsymbol{\epsilon}_t,
\end{aligned} \tag{106}$$

and the Jacobian matrix of (21) can be derived from

$$\begin{aligned}
&h({}^L\mathbf{R}_{I_t}^\top({}^L\mathbf{R}_{G_t}{}^G\mathbf{p}_F + {}^L\mathbf{p}_{G_t} - {}^L\mathbf{p}_{I_t})) \\
&- h({}^L\hat{\mathbf{R}}_{I_t}^\top({}^L\hat{\mathbf{R}}_{G_t}{}^G\mathbf{p}_F + {}^L\hat{\mathbf{p}}_{G_t} - {}^L\hat{\mathbf{p}}_{I_t})) \\
&\approx \nabla h'|_{\hat{\mathfrak{q}}'}(\mathfrak{q}' - \hat{\mathfrak{q}}') \\
&= \nabla h'|_{\hat{\mathfrak{q}}'}\left[{}^L\hat{\mathbf{R}}_{I_t}^\top({}^L\hat{\mathbf{R}}_{I_t}{}^L\mathbf{R}_{I_t}^\top({}^L\mathbf{R}_{G_t}{}^G\mathbf{p}_F + {}^L\mathbf{p}_{G_t} - {}^L\mathbf{p}_{I_t}))\right.
\end{aligned}$$

$$
\begin{aligned}
&-{}^{L}\hat{\mathbf{R}}_{I_t}^{\top}({}^{L}\hat{\mathbf{R}}_{G_t}{}^{G}\mathbf{p}_F + {}^{L}\hat{\mathbf{p}}_{G_t} - {}^{L}\hat{\mathbf{p}}_{I_t})\Big] \\
&= \nabla h'|_{\hat{\mathbf{q}}'}\Big[{}^{L}\hat{\mathbf{R}}_{I_t}^{\top}\Big[{}^{L}\hat{\mathbf{R}}_{I_t}{}^{L}\mathbf{R}_{I_t}^{\top}({}^{L}\mathbf{R}_{G_t}{}^{G}\mathbf{p}_F + {}^{L}\mathbf{p}_{G_t} \\
&-{}^{L}\mathbf{p}_{I_t}) - {}^{L}\hat{\mathbf{R}}_{G_t}{}^{G}\mathbf{p}_F - {}^{L}\hat{\mathbf{p}}_{G_t} + {}^{L}\hat{\mathbf{p}}_{I_t}\Big]\Big] \\
&\approx \nabla h'|_{\hat{\mathbf{q}}'}\Big[{}^{L}\hat{\mathbf{R}}_{I_t}^{\top}\Big[(\mathbf{I}+(\tilde{\boldsymbol{\theta}}_{LI_t})_\times)({}^{L}\mathbf{R}_{G_t}{}^{G}\mathbf{p}_F + {}^{L}\mathbf{p}_{G_t} - {}^{L}\mathbf{p}_{I_t}) \\
&-{}^{L}\hat{\mathbf{R}}_{G_t}{}^{G}\mathbf{p}_F - {}^{L}\hat{\mathbf{p}}_{G_t} + {}^{L}\hat{\mathbf{p}}_{I_t}\Big]\Big] \\
&= \nabla h'|_{\hat{\mathbf{q}}'}{}^{L}\hat{\mathbf{R}}_{I_t}^{\top}\Big[(\mathbf{I}+(\tilde{\boldsymbol{\theta}}_{LI_t})_\times){}^{L}\mathbf{R}_{G_t}{}^{G}\mathbf{p}_F - {}^{L}\hat{\mathbf{R}}_{G_t}{}^{G}\mathbf{p}_F \\
&-\boldsymbol{\xi}_{\mathbf{p}_{LG_t}} + \boldsymbol{\xi}_{\mathbf{p}_{LI_t}}\Big] \\
&\approx \nabla h'|_{\hat{\mathbf{q}}'}{}^{L}\hat{\mathbf{R}}_{I_t}^{\top}\Big[(\mathbf{I}+(\tilde{\boldsymbol{\theta}}_{LI_t})_\times)(\mathbf{I}-(\tilde{\boldsymbol{\theta}}_{LG_t})_\times){}^{L}\hat{\mathbf{R}}_{G_t}{}^{G}\mathbf{p}_F \\
&-{}^{L}\hat{\mathbf{R}}_{G_t}{}^{G}\mathbf{p}_F - \boldsymbol{\xi}_{\mathbf{p}_{LG_t}} + \boldsymbol{\xi}_{\mathbf{p}_{LI_t}}\Big] \\
&\approx \nabla h'|_{\hat{\mathbf{q}}'}{}^{L}\hat{\mathbf{R}}_{I_t}^{\top}\Big[({}^{L}\hat{\mathbf{R}}_{G_t}{}^{G}\mathbf{p}_F)_\times\tilde{\boldsymbol{\theta}}_{LG_t} \\
&-({}^{L}\hat{\mathbf{R}}_{G_t}{}^{G}\mathbf{p}_F)_\times\tilde{\boldsymbol{\theta}}_{LI_t} - \boldsymbol{\xi}_{\mathbf{p}_{LG_t}} + \boldsymbol{\xi}_{\mathbf{p}_{LI_t}}\Big] \\
&= \nabla h'|_{\hat{\mathbf{q}}'}{}^{L}\hat{\mathbf{R}}_{I_t}^{\top}\left[-({}^{L}\hat{\mathbf{R}}_{G_t}{}^{G}\mathbf{p}_F)_\times \quad \mathbf{0}_3 \quad \mathbf{I}_3 \quad \mathbf{0}_3 \quad -\mathbf{I}_3\right. \\
&\left.({}^{L}\hat{\mathbf{R}}_{G_t}{}^{G}\mathbf{p}_F)_\times \quad \mathbf{0}_3 \quad \mathbf{0}_3\right]\boldsymbol{\epsilon}_t. \qquad (107)
\end{aligned}
$$

Further, if the map information is considered as a part of the system state (cf. Sec.V), the observation function of a map landmark ${}^{G}\mathbf{p}_{F_j,t}$ is given by (27) and (28). The Jacobian matrix of (27) can be derived by:

$$
\begin{aligned}
&h({}^{L}\mathbf{R}_{I_t}^{\top}({}^{L}\mathbf{R}_{G_t}{}^{G}\mathbf{p}_{F_j,t} + {}^{L}\mathbf{p}_{G_t} - {}^{L}\mathbf{p}_{I_t})) \\
&- h({}^{L}\hat{\mathbf{R}}_{I_t}^{\top}({}^{L}\hat{\mathbf{R}}_{G_t}{}^{G}\hat{\mathbf{p}}_{F_j,t} + {}^{L}\hat{\mathbf{p}}_{G_t} - {}^{L}\hat{\mathbf{p}}_{I_t})) \\
&\approx \nabla h'|_{\hat{\mathbf{q}}'}{}^{L}\hat{\mathbf{R}}_{I_t}^{\top}\Big[{}^{L}\hat{\mathbf{R}}_{I_t}{}^{L}\mathbf{R}_{I_t}^{\top}({}^{L}\mathbf{R}_{G_t}{}^{G}\mathbf{p}_{F_j,t}) \\
&-{}^{L}\hat{\mathbf{R}}_{G_t}{}^{G}\hat{\mathbf{p}}_{F_j,t} - \boldsymbol{\xi}_{\mathbf{p}_{LG_t}} + \boldsymbol{\xi}_{\mathbf{p}_{LI_t}}\Big] \\
&\approx \nabla h'|_{\hat{\mathbf{q}}'}{}^{L}\hat{\mathbf{R}}_{I_t}^{\top}\Big[(\mathbf{I}+(\tilde{\boldsymbol{\theta}}_{LI_t})_\times)(\mathbf{I}-(\tilde{\boldsymbol{\theta}}_{LG_t})_\times){}^{L}\hat{\mathbf{R}}_{G_t}{}^{G}\mathbf{p}_{F_j,t} \\
&-{}^{L}\hat{\mathbf{R}}_{G_t}{}^{G}\hat{\mathbf{p}}_{F_j,t} - \boldsymbol{\xi}_{\mathbf{p}_{LG_t}} + \boldsymbol{\xi}_{\mathbf{p}_{LI_t}}\Big] \\
&\approx \nabla h'|_{\hat{\mathbf{q}}'}{}^{L}\hat{\mathbf{R}}_{I_t}^{\top}\Big[{}^{L}\hat{\mathbf{R}}_{G_t}({}^{G}\mathbf{p}_{F_j,t} - {}^{G}\hat{\mathbf{p}}_{F_j,t}) - ({}^{L}\hat{\mathbf{R}}_{G_t}{}^{G}\hat{\mathbf{p}}_{F_j,t})_\times\tilde{\boldsymbol{\theta}}_{LI_t} \\
&+({}^{L}\hat{\mathbf{R}}_{G_t}{}^{G}\hat{\mathbf{p}}_{F_j,t})_\times\tilde{\boldsymbol{\theta}}_{LG_t} - \boldsymbol{\xi}_{\mathbf{p}_{LG_t}} + \boldsymbol{\xi}_{\mathbf{p}_{LI_t}}\Big] \\
&= \nabla h'|_{\hat{\mathbf{q}}'}{}^{L}\hat{\mathbf{R}}_{I_t}^{\top}\left[-({}^{L}\hat{\mathbf{R}}_{G_t}{}^{G}\hat{\mathbf{p}}_{F_j,t})_\times \quad \mathbf{0}_3 \quad \mathbf{I}_3 \quad \mathbf{0}_3 \quad -\mathbf{I}_3\right. \\
&\left.({}^{L}\hat{\mathbf{R}}_{G_t}{}^{G}\hat{\mathbf{p}}_{F_j,t})_\times \quad \mathbf{0}_3 \quad \mathbf{0}_3|\cdots\mathbf{0}_3 \quad \mathbf{0}_3\cdots -{}^{L}\hat{\mathbf{R}}_{G_t}\cdots\right]\boldsymbol{\epsilon}_t^*, \qquad (108)
\end{aligned}
$$

which is identical to the Jacobian matrix given in (29).

The Jacobian matrix of (30) is derived from

$$
\begin{aligned}
&h\left[{}^{G}\mathbf{R}_{KF_i,t}^{\top}({}^{G}\mathbf{p}_{F_j,t} - {}^{G}\mathbf{p}_{KF_i,t})\right] \\
&- h\left[{}^{G}\hat{\mathbf{R}}_{KF_i,t}^{\top}({}^{G}\hat{\mathbf{p}}_{F_j,t} - {}^{G}\hat{\mathbf{p}}_{KF_i,t})\right] \\
&\approx \nabla h^*|_{\hat{\mathbf{q}}^*}{}^{G}\hat{\mathbf{R}}_{KF_i,t}^{\top}\Big[{}^{G}\hat{\mathbf{R}}_{KF_i,t}{}^{G}\mathbf{R}_{KF_i,t}^{\top}({}^{G}\mathbf{p}_{F_j,t} - {}^{G}\mathbf{p}_{KF_i,t}) \\
&+{}^{G}\hat{\mathbf{p}}_{KF_i,t} - {}^{G}\hat{\mathbf{p}}_{F_j,t}\Big] \\
&= \nabla h^*|_{\hat{\mathbf{q}}^*}{}^{G}\hat{\mathbf{R}}_{KF_i,t}^{\top}\Big[{}^{G}\hat{\mathbf{R}}_{KF_i,t}{}^{G}\mathbf{R}_{KF_i,t}^{\top}{}^{G}\mathbf{p}_{F_j,t} - {}^{G}\hat{\mathbf{p}}_{F_j,t} \\
&+\boldsymbol{\xi}_{\mathbf{p}_{KF_i,t}}\Big] \\
&\approx \nabla h^*|_{\hat{\mathbf{q}}^*}{}^{G}\hat{\mathbf{R}}_{KF_i,t}^{\top}\Big[(\mathbf{I}+(\tilde{\boldsymbol{\theta}}_{KF_i,t})_\times){}^{G}\mathbf{p}_{F_j,t} - {}^{G}\hat{\mathbf{p}}_{F_j,t} \\
&+\boldsymbol{\xi}_{\mathbf{p}_{KF_i,t}}\Big] \\
&\approx \nabla h^*|_{\hat{\mathbf{q}}^*}{}^{G}\hat{\mathbf{R}}_{KF_i,t}^{\top}\Big[-({}^{G}\hat{\mathbf{p}}_{F_j,t})_\times\tilde{\boldsymbol{\theta}}_{KF_i,t} - \boldsymbol{\xi}_{\mathbf{p}_{F_j,t}} + \boldsymbol{\xi}_{\mathbf{p}_{KF_i,t}}\Big] \\
&= \nabla h^*|_{\hat{\mathbf{q}}^*}{}^{G}\hat{\mathbf{R}}_{KF_i,t}^{\top}\left[\mathbf{0}_3 \quad \mathbf{0}_3 \quad \mathbf{0}_3 \quad \mathbf{0}_3 \quad \mathbf{0}_3\right. \\
&\left.\mathbf{0}_3 \quad \mathbf{0}_3 \quad \mathbf{0}_3|\cdots -({}^{G}\hat{\mathbf{p}}_{F_j,t})_\times \quad \mathbf{I}_3\cdots -\mathbf{I}_3\cdots\right]\boldsymbol{\epsilon}_t^*. \qquad (109)
\end{aligned}
$$

APPENDIX C
PROOF OF LEMMA 3 AND THEOREM 4

For brevity, in the following derivation, all the $\mathbf{0}$ and $\mathbf{I}$ without the subscript are the 3×3 matrices.

Propagation matrix: With the state definition of (31), and the propagation functions (12). Similar to the derivation of [10], we can get that the state transition matrix is:

$$
{}^{st}\boldsymbol{\Phi}_{t+1|t} = \begin{bmatrix}
{}^{st}\boldsymbol{\Phi}_1 & \mathbf{0} & \mathbf{0} & \mathbf{0} & \mathbf{0} & \mathbf{0} \\
{}^{st}\boldsymbol{\Phi}_2 & \mathbf{I} & \mathbf{0} & \mathbf{0} & \mathbf{0} & \mathbf{0} \\
{}^{st}\boldsymbol{\Phi}_3 & \mathbf{I}\Delta & \mathbf{I} & \mathbf{0} & \mathbf{0} & \mathbf{0} \\
\mathbf{0} & \mathbf{0} & \mathbf{0} & \mathbf{I} & \mathbf{0} & \mathbf{0} \\
\mathbf{0} & \mathbf{0} & \mathbf{0} & \mathbf{0} & \mathbf{I} & \mathbf{0} \\
\mathbf{0} & \mathbf{0} & \mathbf{0} & \mathbf{0} & \mathbf{0} & \mathbf{I}
\end{bmatrix}, \qquad (110)
$$

where

$$
\begin{aligned}
{}^{st}\boldsymbol{\Phi}_1 &= {}^{L}\hat{\mathbf{R}}_{I_{t+1}}^{\top}{}^{L}\hat{\mathbf{R}}_{I_t}, \\
{}^{st}\boldsymbol{\Phi}_2 &= -({}^{L}\hat{\mathbf{v}}_{I_{t+1}} - {}^{L}\hat{\mathbf{v}}_{I_t} + \mathbf{g}\Delta)_\times{}^{L}\hat{\mathbf{R}}_{I_t}, \\
{}^{st}\boldsymbol{\Phi}_3 &= -({}^{L}\hat{\mathbf{p}}_{I_{t+1}} - {}^{L}\hat{\mathbf{p}}_{I_t} - {}^{L}\hat{\mathbf{v}}_{I_t}\Delta + \frac{1}{2}\mathbf{g}\Delta^2)_\times{}^{L}\hat{\mathbf{R}}_{I_t}.
\end{aligned}
$$

Δ is one time step from timestamp t to timestamp $t+1$.

Jacobian matrix of local feature measurements: For the local feature based observation function (19), the Jacobian matrix is given as

$$
{}^{st}\mathbf{H}_{L_t} = {}^{st}\mathbf{H}_{\pi_t}\left[{}^{st}\mathbf{H}_{L1} \quad \mathbf{0} \quad -{}^{L}\hat{\mathbf{R}}_{I_t}^{\top} \quad {}^{L}\hat{\mathbf{R}}_{I_t}^{\top} \quad \mathbf{0} \quad \mathbf{0}\right], \qquad (111)
$$

where ${}^{st}\mathbf{H}_{\pi_t}$ is the Jacobians of the projection function and

$$
{}^{st}\mathbf{H}_{L1} = ({}^{L}\hat{\mathbf{R}}_{I_t}^{\top}({}^{L}\hat{\mathbf{p}}_{f_t} - {}^{L}\hat{\mathbf{p}}_{I_t}))_\times.
$$

Jacobian matrix of map based measurements: For the map based observation function (21), the Jacobian matrix is given as

$$
{}^{st}\mathbf{H}_{G_t} = {}^{st}\mathbf{H}'_{\pi_t}\left[{}^{st}\mathbf{H}_{G1} \quad \mathbf{0} \quad -{}^{L}\hat{\mathbf{R}}_{I_t}^{\top} \quad \mathbf{0} \quad {}^{st}\mathbf{H}_{G2} \quad {}^{L}\hat{\mathbf{R}}_{I_t}^{\top}\right], \qquad (112)
$$

where ${}^{st}\mathbf{H}'_{\pi_t}$ is the Jacobians of the projection function, the superscript $'$ is just for distinguishing from local observation, and

$$
\begin{aligned}
{}^{st}\mathbf{H}_{G1} &= \left[{}^{L}\hat{\mathbf{R}}_{I_t}^{\top}({}^{L}\hat{\mathbf{R}}_{G_t}{}^{G}\mathbf{p}_F + {}^{L}\hat{\mathbf{p}}_{G_t} - {}^{L}\hat{\mathbf{p}}_{I_t})\right]_\times, \\
{}^{st}\mathbf{H}_{G2} &= -{}^{L}\hat{\mathbf{R}}_{I_t}^{\top}{}^{L}\hat{\mathbf{R}}_{G_t}({}^{G}\mathbf{p}_F)_\times.
\end{aligned}
$$

Observability matrix: Assume at time step $t-1$, we have a state denoted as $\mathbf{X}_{t-1|t-1}$. After propagation, we get the state $\mathbf{X}_{t|t-1}$. After update, we get the state at time step t, i.e. $\mathbf{X}_{t|t}$.

The following derivation fall into two cases: (a) one is that the prediction state $\mathbf{X}_{t|t-1}$ is equal to update state $\mathbf{X}_{t|t}$, which is ideal situation. In this situation, we denote both $\mathbf{X}_{t|t-1}$ and $\mathbf{X}_{t|t}$ as $\mathbf{X}_t$. (b) The other one is that the prediction state $\mathbf{X}_{t|t-1}$ is not equal to update state $\mathbf{X}_{t|t}$.

• For case (a):

$$
\begin{aligned}
{}^{st}\mathbf{\Phi}_{t|0} &= {}^{st}\mathbf{\Phi}_{t|t-1}\cdots{}^{st}\mathbf{\Phi}_{2|1}{}^{st}\mathbf{\Phi}_{1|0} \\
&= \begin{bmatrix} {}^{st}\mathbf{\Phi}(1) & \mathbf{0} & \mathbf{0} & \mathbf{0} & \mathbf{0} & \mathbf{0} \\ {}^{st}\mathbf{\Phi}(2) & \mathbf{I} & \mathbf{0} & \mathbf{0} & \mathbf{0} & \mathbf{0} \\ {}^{st}\mathbf{\Phi}(3) & \mathbf{I}\Delta_t & \mathbf{I} & \mathbf{0} & \mathbf{0} & \mathbf{0} \\ \mathbf{0} & \mathbf{0} & \mathbf{0} & \mathbf{I} & \mathbf{0} & \mathbf{0} \\ \mathbf{0} & \mathbf{0} & \mathbf{0} & \mathbf{0} & \mathbf{I} & \mathbf{0} \\ \mathbf{0} & \mathbf{0} & \mathbf{0} & \mathbf{0} & \mathbf{0} & \mathbf{I} \end{bmatrix},
\end{aligned} \tag{113}
$$

where Δ_t is t time steps from timestamp 0 to timestamp t,

$$
\begin{aligned}
{}^{st}\mathbf{\Phi}(1) &= {}^{L}\hat{\mathbf{R}}_{I_t}^{\top}{}^{L}\hat{\mathbf{R}}_{I_0}, \\
{}^{st}\mathbf{\Phi}(2) &= -({}^{L}\hat{\mathbf{v}}_{I_t} - {}^{L}\hat{\mathbf{v}}_{I_0} + \mathbf{g}\Delta_t)_{\times}{}^{L}\hat{\mathbf{R}}_{I_0}, \\
{}^{st}\mathbf{\Phi}(3) &= -({}^{L}\hat{\mathbf{p}}_{I_t} - {}^{L}\hat{\mathbf{p}}_{I_0} - {}^{L}\hat{\mathbf{v}}_{I_0}\Delta_t + \frac{1}{2}\mathbf{g}\Delta_t^2)_{\times}{}^{L}\hat{\mathbf{R}}_{I_0}.
\end{aligned}
$$

Taking (111),(112) and (113) into (33), we have the following expressions for $i = 1, \cdots, t$:

$$
\begin{aligned}
{}^{st}\mathbf{M}_{L_i} = {}^{st}\mathbf{H}_{\pi_i}[&{}^{st}\mathbf{M}_{L_i}(1) \quad -{}^{L}\hat{\mathbf{R}}_{I_i}^{\top}\Delta_i \quad -{}^{L}\hat{\mathbf{R}}_{I_i}^{\top} \quad {}^{L}\hat{\mathbf{R}}_{I_i}^{\top} \\
&\mathbf{0} \quad \mathbf{0}],
\end{aligned} \tag{114}
$$

$$
\begin{aligned}
{}^{st}\mathbf{M}_{G_i} = {}^{st}\mathbf{H}'_{\pi_i}[&{}^{st}\mathbf{M}_{G_i}(1) \quad -{}^{L}\hat{\mathbf{R}}_{I_i}^{\top}\Delta_i \quad -{}^{L}\hat{\mathbf{R}}_{I_i}^{\top} \quad \mathbf{0} \\
&{}^{st}\mathbf{M}_{G_i}(2) \quad {}^{L}\hat{\mathbf{R}}_{I_i}^{\top}],
\end{aligned} \tag{115}
$$

where

$$
\begin{aligned}
{}^{st}\mathbf{M}_{L_i}(1) &= {}^{L}\hat{\mathbf{R}}_{I_i}^{\top}({}^{L}\hat{\mathbf{p}}_{f_i} - {}^{L}\hat{\mathbf{p}}_{I_0} - {}^{L}\hat{\mathbf{v}}_{I_0}\Delta_i + \frac{1}{2}\mathbf{g}\Delta_i^2)_{\times}{}^{L}\hat{\mathbf{R}}_{I_0}, \\
{}^{st}\mathbf{M}_{G_i}(1) &= {}^{L}\hat{\mathbf{R}}_{I_i}^{\top}({}^{L}\hat{\mathbf{R}}_{G_i}{}^{G}\mathbf{p}_F + {}^{L}\hat{\mathbf{p}}_{G_i} - {}^{L}\hat{\mathbf{p}}_{I_0} - {}^{L}\hat{\mathbf{v}}_{I_0}\Delta_i \\
&\quad + \frac{1}{2}\mathbf{g}\Delta_i^2)_{\times}{}^{L}\hat{\mathbf{R}}_{I_0}, \\
{}^{st}\mathbf{M}_{G_i}(2) &= -{}^{L}\hat{\mathbf{R}}_{I_i}^{\top}{}^{L}\hat{\mathbf{R}}_{G_i}({}^{G}\mathbf{p}_F)_{\times}.
\end{aligned}
$$

Noting that in case (a), for each timestamp, the state value after propagation is the same as the state value after update, i.e. for the state elements whose differential equation equal to zero, i.e.,${}^{L}\mathbf{p}_f$, ${}^{L}\mathbf{R}_G$, and ${}^{L}\mathbf{p}_G$, their values are always equal to their initial values. Therefore, in the observability matrix above, ${}^{L}\hat{\mathbf{R}}_{G_0} = {}^{L}\hat{\mathbf{R}}_{G_1} = \cdots = {}^{L}\hat{\mathbf{R}}_{G_t} \triangleq {}^{L}\mathbf{R}_G$, so as ${}^{L}\mathbf{p}_f, {}^{L}\mathbf{p}_G$.

From above observability matrix, we can find that its null space would be

$$
\text{Null}(\mathbf{M}) = \begin{bmatrix} {}^{L}\hat{\mathbf{R}}_{I_0}^{\top}\mathbf{g} & \mathbf{0}_3 \\ -({}^{L}\hat{\mathbf{v}}_{I_0})_{\times}\mathbf{g} & \mathbf{0}_3 \\ -({}^{L}\hat{\mathbf{p}}_{I_0})_{\times}\mathbf{g} & \mathbf{I}_3 \\ -({}^{L}\hat{\mathbf{p}}_{f})_{\times}\mathbf{g} & \mathbf{I}_3 \\ {}^{L}\mathbf{R}_G^{\top}\mathbf{g} & \mathbf{0}_3 \\ -({}^{L}\mathbf{p}_G)_{\times}\mathbf{g} & \mathbf{I}_3 \end{bmatrix}, \tag{116}
$$

whose dimension is four, so that **Lemma 3** is proved.

It is worth mentioning that from (114) and (115), readers can find another right null space of ${}^{st}\mathbf{M}$ except (116):

$$
\begin{bmatrix} \mathbf{0}_3 \\ \mathbf{0}_3 \\ \mathbf{0}_3 \\ \mathbf{0}_3 \\ \mathbf{I}_3 \\ {}^{L}\mathbf{R}_G({}^{G}\mathbf{p}_F)_{\times} \end{bmatrix}. \tag{117}
$$

This is because we only consider one map feature ${}^{G}\mathbf{p}_F$. However, in practice, a map keyframe will observe many features. If there are three or more non-collinear features observed by the map keyframe, the right null space given by (117) vanishes. The similar situation will be encountered in the following analyses in Appendix D, Appendix E and Appendix F. Therefore, in the following context, we assume there are three or more non-collinear map features when deriving the right null space of the observability matrix, whereas only one map feature is considered when deriving Jacobian matrices.

• For case (b): In this situation, the predicted state value is usually not equal with the updated state value. Therefore, the first three columns of the transition matrix $\mathbf{\Phi}_{t|0}$ do not have the elegant form as (113). On the other hand, for case (b), the estimated ${}^{L}\hat{\mathbf{R}}_{G_0} \neq {}^{L}\hat{\mathbf{R}}_{G_1} \neq {}^{L}\hat{\mathbf{R}}_{G_t}$, so as ${}^{L}\hat{\mathbf{p}}_{G_t}$ and ${}^{L}\hat{\mathbf{p}}_{f_t}$. Therefore, the first column of (116) will not be the null space of the observability matrix, and the dimension of the right null space of the observability matrix is three, which is in accordance with **Theorem 4**.

APPENDIX D
PROOF OF THEOREM 5

With (13), the discrete-time state transition matrix can be represented by the matrix exponential map:

$$
\begin{aligned}
{}^{in}\mathbf{\Phi}_{t+1|t} = \exp_m(\mathbf{A}_{\mathbf{X}_{A_t}}\Delta) &= \mathbf{I} + \mathbf{A}_{\mathbf{X}_{A_t}}\Delta + \frac{1}{2!}\mathbf{A}_{\mathbf{X}_{A_t}}^2\Delta^2 \\
&\quad + \frac{1}{3!}\mathbf{A}_{\mathbf{X}_{A_t}}^3\Delta^3 + \cdots,
\end{aligned} \tag{118}
$$

where Δ is one time step from timestamp t to timestamp $t+1$.

Fortunately, $\mathbf{A}_{\mathbf{X}_{A_t}}$ is a nilpotent matrix with the degree of three, i.e. $\mathbf{A}_{\mathbf{X}_{A_t}}^3 = \mathbf{0}$, so that we have:

$$
{}^{in}\mathbf{\Phi}_{t+1|t} = \begin{bmatrix} \mathbf{I} & \mathbf{0} & \mathbf{0} & \mathbf{0} & \mathbf{0} & \mathbf{0} \\ (\mathbf{g})_{\times}\Delta & \mathbf{I} & \mathbf{0} & \mathbf{0} & \mathbf{0} & \mathbf{0} \\ \frac{1}{2}(\mathbf{g})_{\times}\Delta^2 & \mathbf{I}\Delta & \mathbf{I} & \mathbf{0} & \mathbf{0} & \mathbf{0} \\ \mathbf{0} & \mathbf{0} & \mathbf{0} & \mathbf{I} & \mathbf{0} & \mathbf{0} \\ \mathbf{0} & \mathbf{0} & \mathbf{0} & \mathbf{0} & \mathbf{I} & \mathbf{0} \\ \mathbf{0} & \mathbf{0} & \mathbf{0} & \mathbf{0} & \mathbf{0} & \mathbf{I} \end{bmatrix}. \tag{119}
$$

All the $\mathbf{0}$ and $\mathbf{I}$ in (119) are 3×3 matrices. Similarly, $\mathbf{A}_t$ is a nilpotent matrix with the degree of four.

Substituting (119) into (32), we have

$$
{}^{in}\mathbf{\Phi}_{t|0} = \begin{bmatrix} \mathbf{I} & \mathbf{0} & \mathbf{0} & \mathbf{0} & \mathbf{0} & \mathbf{0} \\ (\mathbf{g})_{\times}\Delta_t & \mathbf{I} & \mathbf{0} & \mathbf{0} & \mathbf{0} & \mathbf{0} \\ \frac{1}{2}(\mathbf{g})_{\times}\Delta_t^2 & \mathbf{I}\Delta_t & \mathbf{I} & \mathbf{0} & \mathbf{0} & \mathbf{0} \\ \mathbf{0} & \mathbf{0} & \mathbf{0} & \mathbf{I} & \mathbf{0} & \mathbf{0} \\ \mathbf{0} & \mathbf{0} & \mathbf{0} & \mathbf{0} & \mathbf{I} & \mathbf{0} \\ \mathbf{0} & \mathbf{0} & \mathbf{0} & \mathbf{0} & \mathbf{0} & \mathbf{I} \end{bmatrix}. \tag{120}
$$

For the Jacobian matrix of observation function, with (20) and (22), neglecting the IMU bias parts, we have

$$
\begin{aligned}
{}^{in}\mathbf{H}_{L_t} &= \mathbf{H}_{L_t}, \\
{}^{in}\mathbf{H}_{G_t} &= \mathbf{H}_{G_t}.
\end{aligned} \tag{121}
$$

Taking (120) and (121) into (33), we have the following expressions for $i = 1, \cdots, t$:

$$
\begin{aligned}
{}^{in}\mathbf{M}_{L_i} &= -\nabla h|_{\hat{\mathfrak{q}}}\, {}^{L}\hat{\mathbf{R}}_{I_i}^{\top}[\frac{1}{2}(\mathbf{g})_{\times}\Delta_i{}^2 \quad \mathbf{I}_3\Delta_i \quad \mathbf{I}_3 \quad -\mathbf{I}_3 \\
&\qquad \mathbf{0}_3 \quad \mathbf{0}_3], \\
{}^{in}\mathbf{M}_{G_i} &= -\nabla h'|_{\hat{\mathfrak{q}}'}\, {}^{L}\hat{\mathbf{R}}_{I_i}^{\top}[-({}^{L}\hat{\mathbf{R}}_{G_i}\, {}^{G}\mathbf{p}_F)_{\times} + \frac{1}{2}(\mathbf{g})_{\times}\Delta_i^2 \quad \mathbf{I}_3\Delta_i \\
&\qquad \mathbf{I}_3 \quad \mathbf{0}_3 \quad -\mathbf{I}_3 \quad ({}^{L}\hat{\mathbf{R}}_{G_i}\, {}^{G}\mathbf{p}_F)_{\times}].
\end{aligned} \tag{122}
$$

Readers can verify that (36) is the right null space of ${}^{in}\mathbf{M}$, which is independent from the state estimation. Therefore, our proposed invariant EKF can naturally maintain the correct dimension of the unobservable subspace of the *perfect augmented system*.

Appendix E
Proof of Theorem 6

For ease of understanding, it is recommended that the readers read the following paragraphs in comparison with Appendix C.

As the map information is supposed to be static, the corresponding part of the propagation matrix should be identity. Therefore, we can get the state transition matrix as

$$
{}^{st}\mathbf{\Phi}^*_{t+1|t} = \left[\begin{array}{ccccccccc}
{}^{st}\mathbf{\Phi}_1 & \mathbf{0} & \mathbf{0} & \mathbf{0} & \mathbf{0} & \mathbf{0} & \mathbf{0} & \mathbf{0} & \mathbf{0} \\
{}^{st}\mathbf{\Phi}_2 & \mathbf{I} & \mathbf{0} & \mathbf{0} & \mathbf{0} & \mathbf{0} & \mathbf{0} & \mathbf{0} & \mathbf{0} \\
{}^{st}\mathbf{\Phi}_3 & \mathbf{I}\Delta & \mathbf{I} & \mathbf{0} & \mathbf{0} & \mathbf{0} & \mathbf{0} & \mathbf{0} & \mathbf{0} \\
\mathbf{0} & \mathbf{0} & \mathbf{0} & \mathbf{I} & \mathbf{0} & \mathbf{0} & \mathbf{0} & \mathbf{0} & \mathbf{0} \\
\mathbf{0} & \mathbf{0} & \mathbf{0} & \mathbf{0} & \mathbf{I} & \mathbf{0} & \mathbf{0} & \mathbf{0} & \mathbf{0} \\
\mathbf{0} & \mathbf{0} & \mathbf{0} & \mathbf{0} & \mathbf{0} & \mathbf{I} & \mathbf{0} & \mathbf{0} & \mathbf{0} \\
\hline
\mathbf{0} & \mathbf{0} & \mathbf{0} & \mathbf{0} & \mathbf{0} & \mathbf{0} & \mathbf{I} & \mathbf{0} & \mathbf{0} \\
\mathbf{0} & \mathbf{0} & \mathbf{0} & \mathbf{0} & \mathbf{0} & \mathbf{0} & \mathbf{0} & \mathbf{I} & \mathbf{0} \\
\mathbf{0} & \mathbf{0} & \mathbf{0} & \mathbf{0} & \mathbf{0} & \mathbf{0} & \mathbf{0} & \mathbf{0} & \mathbf{I}
\end{array}\right], \tag{123}
$$

where ${}^{st}\mathbf{\Phi}_1, {}^{st}\mathbf{\Phi}_2, {}^{st}\mathbf{\Phi}_3$ are defined in (110).

As the local observation function is not involved with map information, the Jacobian matrix of the local observation function is identical to that in Appendix C. For the global observation, there are two kinds of functions (cf. (27) and (28))[1].

The Jacobian matrix of (27) with standard EKF is given by

$$
\begin{aligned}
{}^{st}\mathbf{H}^*_{G_t,C} = {}^{st}\mathbf{H}'_{\pi_t,C} \big[& {}^{st}\mathbf{H}^*_{G1} \quad \mathbf{0} \quad -{}^{L}\hat{\mathbf{R}}_{I_t}^{\top} \quad \mathbf{0} \quad {}^{st}\mathbf{H}^*_{G2} \\
& {}^{L}\hat{\mathbf{R}}_{I_t}^{\top}| \quad \mathbf{0} \quad \mathbf{0} \quad {}^{L}\hat{\mathbf{R}}_{I_t}^{\top}{}^{L}\hat{\mathbf{R}}_{G_t}\big],
\end{aligned} \tag{124}
$$

where ${}^{st}\mathbf{H}'_{\pi_t,C}$ is the Jacobians of the projection function. The superscript $'$ is just for distinguishing from local observation.

$$
\begin{aligned}
{}^{st}\mathbf{H}^*_{G1} &= \left[{}^{L}\hat{\mathbf{R}}_{I_t}^{\top}({}^{L}\hat{\mathbf{R}}_{G_t}\, {}^{G}\hat{\mathbf{p}}_{F,t} + {}^{L}\hat{\mathbf{p}}_{G_t} - {}^{L}\hat{\mathbf{p}}_{I_t})\right]_{\times}, \\
{}^{st}\mathbf{H}^*_{G2} &= -{}^{L}\hat{\mathbf{R}}_{I_t}^{\top}{}^{L}\hat{\mathbf{R}}_{G_t}({}^{G}\hat{\mathbf{p}}_{F,t})_{\times}.
\end{aligned}
$$

[1]Here, we neglect the IMU bias parts of (29) and (30) for simplicity. Besides, only one map keyframe and one map landmark are considered, such that ${}^{G}\hat{\mathbf{p}}_{F_j,t}$ in (29) and (30) is simplified as ${}^{G}\hat{\mathbf{p}}_{F,t}$, and ${}^{G}\hat{\mathbf{R}}_{KF_i,t}$ is simplified as ${}^{G}\hat{\mathbf{R}}_{KF,t}$

The Jacobian matrix of (28) with standard EKF is given by

$$
\begin{aligned}
{}^{st}\mathbf{H}^*_{G_t,KF} = {}^{st}\mathbf{H}'_{\pi_t,KF} \big[& \mathbf{0} \quad \mathbf{0} \quad \mathbf{0} \quad \mathbf{0} \quad \mathbf{0} \quad \mathbf{0}| \\
& \left[{}^{G}\hat{\mathbf{R}}_{KF,t}^{\top}({}^{G}\hat{\mathbf{p}}_{F,t} - {}^{G}\hat{\mathbf{p}}_{KF,t})\right]_{\times} \quad -{}^{G}\hat{\mathbf{R}}_{KF,t}^{\top} \quad {}^{G}\hat{\mathbf{R}}_{KF,t}^{\top}\big].
\end{aligned} \tag{125}
$$

Therefore the Jacobian matrix of map based measurements is

$$
{}^{st}\mathbf{H}^*_{G_t} = \begin{bmatrix} {}^{st}\mathbf{H}^*_{G_t,C} \\ {}^{st}\mathbf{H}^*_{G_t,KF} \end{bmatrix}. \tag{126}
$$

Follow the procedure of Appendix C.

• For the ideal case, the components of the observability matrix ${}^{st}\mathbf{M}^*$ are given by

$$
\begin{aligned}
{}^{st}\mathbf{M}^*_{L_i} = {}^{st}\mathbf{H}_{\pi_i}[& {}^{st}\mathbf{M}^*_{L_i}(1) \quad -{}^{L}\hat{\mathbf{R}}_{I_i}^{\top}\Delta_i \quad -{}^{L}\hat{\mathbf{R}}_{I_i}^{\top} \quad {}^{L}\hat{\mathbf{R}}_{I_i}^{\top} \\
& \mathbf{0} \quad \mathbf{0}| \quad \mathbf{0} \quad \mathbf{0} \quad \mathbf{0}],
\end{aligned}
$$

$$
\begin{aligned}
{}^{st}\mathbf{M}^*_{G_i,C} = {}^{st}\mathbf{H}'_{\pi_i,C}[& {}^{st}\mathbf{M}^*_{G_i}(1) \quad -{}^{L}\hat{\mathbf{R}}_{I_i}^{\top}\Delta_i \quad -{}^{L}\hat{\mathbf{R}}_{I_i}^{\top} \quad \mathbf{0} \\
& {}^{st}\mathbf{M}^*_{G_i}(2) \quad {}^{L}\hat{\mathbf{R}}_{I_i}^{\top}| \quad \mathbf{0} \quad \mathbf{0} \quad {}^{L}\hat{\mathbf{R}}_{I_i}^{\top}{}^{L}\hat{\mathbf{R}}_{G_i}],
\end{aligned}
$$

$$
\begin{aligned}
{}^{st}\mathbf{M}^*_{G_i,KF} = {}^{st}\mathbf{H}'_{\pi_i,KF}[& \mathbf{0} \quad \mathbf{0} \quad \mathbf{0} \quad \mathbf{0} \quad \mathbf{0} \quad \mathbf{0}| \\
& {}^{st}\mathbf{M}^*_{G_i}(3) \quad -{}^{G}\hat{\mathbf{R}}_{KF,i}^{\top} \quad {}^{G}\hat{\mathbf{R}}_{KF,i}^{\top}],
\end{aligned}
$$

$$
{}^{st}\mathbf{M}^*_{G_i} = \begin{bmatrix} {}^{st}\mathbf{M}^*_{G_i,C} \\ {}^{st}\mathbf{M}^*_{G_i,KF} \end{bmatrix},
$$

where $i = 1, \cdots, t$, and

$$
\begin{aligned}
{}^{st}\mathbf{M}^*_{L_i}(1) &= {}^{L}\hat{\mathbf{R}}_{I_i}^{\top}({}^{L}\hat{\mathbf{p}}_{f_i} - {}^{L}\hat{\mathbf{p}}_{I_0} - {}^{L}\hat{\mathbf{v}}_{I_0}\Delta_i + \frac{1}{2}\mathbf{g}\Delta_i^2)_{\times}{}^{L}\hat{\mathbf{R}}_{I_0}, \\
{}^{st}\mathbf{M}^*_{G_i}(1) &= {}^{L}\hat{\mathbf{R}}_{I_i}^{\top}({}^{L}\hat{\mathbf{R}}_{G_i}\, {}^{G}\hat{\mathbf{p}}_{F,i} + {}^{L}\hat{\mathbf{p}}_{G_i} - {}^{L}\hat{\mathbf{p}}_{I_0} - {}^{L}\hat{\mathbf{v}}_{I_0}\Delta_i \\
&\quad + \frac{1}{2}\mathbf{g}\Delta_i^2)_{\times}{}^{L}\hat{\mathbf{R}}_{I_0}, \\
{}^{st}\mathbf{M}^*_{G_i}(2) &= -{}^{L}\hat{\mathbf{R}}_{I_i}^{\top}{}^{L}\hat{\mathbf{R}}_{G_i}({}^{G}\hat{\mathbf{p}}_{F,i})_{\times}, \\
{}^{st}\mathbf{M}^*_{G_i}(3) &= \left[{}^{G}\hat{\mathbf{R}}_{KF,i}^{\top}({}^{G}\hat{\mathbf{p}}_{F,i} - {}^{G}\hat{\mathbf{p}}_{KF,i})\right]_{\times}.
\end{aligned}
$$

Noting that for the ideal case, all the map-related variables do not change over timestamp. Therefore, ${}^{G}\hat{\mathbf{R}}_{KF,0} = {}^{G}\hat{\mathbf{R}}_{KF,1} = \cdots = {}^{G}\hat{\mathbf{R}}_{KF,t} \triangleq {}^{G}\mathbf{R}_{KF}$, so as ${}^{G}\mathbf{p}_{KF}, {}^{G}\mathbf{p}_F$. At this point, readers can verify that (38) is the right null space of the observability matrix ${}^{st}\mathbf{M}^*$ for the ideal case.

Appendix F
Proof of Theorem 8

Following the derivation of the Appendix D, we can get the state transition matrix as

$$
{}^{in}\mathbf{\Phi}^*_{t+1|t} = \left[\begin{array}{ccccccccc}
\mathbf{I} & \mathbf{0} & \mathbf{0} & \mathbf{0} & \mathbf{0} & \mathbf{0} & \mathbf{0} & \mathbf{0} & \mathbf{0} \\
(\mathbf{g})_{\times}\Delta & \mathbf{I} & \mathbf{0} & \mathbf{0} & \mathbf{0} & \mathbf{0} & \mathbf{0} & \mathbf{0} & \mathbf{0} \\
\frac{1}{2}(\mathbf{g})_{\times}\Delta^2 & \mathbf{I}\Delta & \mathbf{I} & \mathbf{0} & \mathbf{0} & \mathbf{0} & \mathbf{0} & \mathbf{0} & \mathbf{0} \\
\mathbf{0} & \mathbf{0} & \mathbf{0} & \mathbf{I} & \mathbf{0} & \mathbf{0} & \mathbf{0} & \mathbf{0} & \mathbf{0} \\
\mathbf{0} & \mathbf{0} & \mathbf{0} & \mathbf{0} & \mathbf{I} & \mathbf{0} & \mathbf{0} & \mathbf{0} & \mathbf{0} \\
\mathbf{0} & \mathbf{0} & \mathbf{0} & \mathbf{0} & \mathbf{0} & \mathbf{I} & \mathbf{0} & \mathbf{0} & \mathbf{0} \\
\hline
\mathbf{0} & \mathbf{0} & \mathbf{0} & \mathbf{0} & \mathbf{0} & \mathbf{0} & \mathbf{I} & \mathbf{0} & \mathbf{0} \\
\mathbf{0} & \mathbf{0} & \mathbf{0} & \mathbf{0} & \mathbf{0} & \mathbf{0} & \mathbf{0} & \mathbf{I} & \mathbf{0} \\
\mathbf{0} & \mathbf{0} & \mathbf{0} & \mathbf{0} & \mathbf{0} & \mathbf{0} & \mathbf{0} & \mathbf{0} & \mathbf{I}
\end{array}\right], \tag{127}
$$

and

$$
{}^{in}\mathbf{\Phi}^*_{t|0} = \left[\begin{array}{cccccc|ccc}
\mathbf{I} & \mathbf{0} & \mathbf{0} & \mathbf{0} & \mathbf{0} & \mathbf{0} & \mathbf{0} & \mathbf{0} & \mathbf{0} \\
(\mathbf{g})_\times \Delta_t & \mathbf{I} & \mathbf{0} & \mathbf{0} & \mathbf{0} & \mathbf{0} & \mathbf{0} & \mathbf{0} & \mathbf{0} \\
\frac{1}{2}(\mathbf{g})_\times \Delta_t^2 & \mathbf{I}\Delta_t & \mathbf{I} & \mathbf{0} & \mathbf{0} & \mathbf{0} & \mathbf{0} & \mathbf{0} & \mathbf{0} \\
\mathbf{0} & \mathbf{0} & \mathbf{0} & \mathbf{I} & \mathbf{0} & \mathbf{0} & \mathbf{0} & \mathbf{0} & \mathbf{0} \\
\mathbf{0} & \mathbf{0} & \mathbf{0} & \mathbf{0} & \mathbf{I} & \mathbf{0} & \mathbf{0} & \mathbf{0} & \mathbf{0} \\
\mathbf{0} & \mathbf{0} & \mathbf{0} & \mathbf{0} & \mathbf{0} & \mathbf{I} & \mathbf{0} & \mathbf{0} & \mathbf{0} \\
\hline
\mathbf{0} & \mathbf{0} & \mathbf{0} & \mathbf{0} & \mathbf{0} & \mathbf{0} & \mathbf{I} & \mathbf{0} & \mathbf{0} \\
\mathbf{0} & \mathbf{0} & \mathbf{0} & \mathbf{0} & \mathbf{0} & \mathbf{0} & \mathbf{0} & \mathbf{I} & \mathbf{0} \\
\mathbf{0} & \mathbf{0} & \mathbf{0} & \mathbf{0} & \mathbf{0} & \mathbf{0} & \mathbf{0} & \mathbf{0} & \mathbf{I}
\end{array}\right], \tag{128}
$$

With the Jacobian matrices of local/map feature based observation functions given by (20), (29) and (30)[2], the components of the observability matrix ${}^{in}\mathbf{M}^*$ is given by

$$
\begin{aligned}
{}^{in}\mathbf{M}^*_{L_i} &= -\nabla h|_{\hat{\mathfrak{q}}}\, {}^{L}\hat{\mathbf{R}}_{I_i}^\top [\frac{1}{2}(\mathbf{g})_\times \Delta_i{}^2 \quad \mathbf{I}_3\Delta_i \quad \mathbf{I}_3 \quad -\mathbf{I}_3 \\
&\quad \mathbf{0}_3 \quad \mathbf{0}_3 | \quad \mathbf{0}_3 \quad \mathbf{0}_3 \quad \mathbf{0}_3], \\
{}^{in}\mathbf{M}^*_{G_i,C} &= -\nabla h'|_{\hat{\mathfrak{q}}'}\, {}^{L}\hat{\mathbf{R}}_{I_i}^\top [-({}^{L}\hat{\mathbf{R}}_{G_i}\, {}^{G}\hat{\mathbf{p}}_{F,i})_\times + \frac{1}{2}(\mathbf{g})_\times \Delta_i^2 \\
&\quad \mathbf{I}_3\Delta_i \quad \mathbf{I}_3 \quad \mathbf{0}_3 \quad -\mathbf{I}_3 \quad ({}^{L}\hat{\mathbf{R}}_{G_i}\, {}^{G}\hat{\mathbf{p}}_{F,i})_\times | \quad \mathbf{0}_3 \quad \mathbf{0}_3 \quad -{}^{L}\hat{\mathbf{R}}_{G_i}], \\
{}^{in}\mathbf{M}^*_{G_i,KF} &= -\nabla h^*|_{\hat{\mathfrak{q}}^*}\, {}^{G}\hat{\mathbf{R}}_{KF,i}^\top [\mathbf{0}_3 \quad \mathbf{0}_3 \quad \mathbf{0}_3 \quad \mathbf{0}_3 \quad \mathbf{0}_3 \\
&\quad \mathbf{0}_3 \quad \mathbf{0}_3 \quad \mathbf{0}_3 | -({}^{G}\hat{\mathbf{p}}_{F_i})_\times \quad \mathbf{I}_3 \quad -\mathbf{I}_3].
\end{aligned} \tag{129}
$$

Again, for the ideal case, all the map-related variables do not change over timestamp. Therefore, ${}^{G}\hat{\mathbf{R}}_{KF,0} = {}^{G}\hat{\mathbf{R}}_{KF,1} = \cdots = {}^{G}\hat{\mathbf{R}}_{KF,t} \triangleq {}^{G}\mathbf{R}_{KF}$, so as ${}^{G}\mathbf{p}_{KF}, {}^{G}\mathbf{p}_{F}$. At this point, readers can verify that (40) is the right null space of the observability matrix ${}^{in}\mathbf{M}^*$ for the ideal case.

Appendix G
Simulation Results under Four different Scenarios

This section performs additional simulations to validate the consistency and effectiveness of our proposed algorithm. The map (blue) trajectory and test (orange) trajectory given in Fig. 12 are the same as those in the main paper. However, besides the simulation scenario of the main paper (Scenario 2), this section gives another three scenarios (Scenario 1, 3, 4). From Scenario 1 to Scenario 4, the matching information is from dense to sparse, so that we can see how the number of feature matches influences the performance of the algorithms.

-Scenario 1:

In this scenario, the robot will repeat the orange trajectory ten times for each run. So the total running distance is around $10 \times 128m = 1280m$. The locations where feature matches between the map and the running VIO occur are marked in Fig. 12 (a) by black asterisks (20 locations for each loop). During the ten loops of each run, the feature matching always occurs for each loop (200 locations).

-Scenario 2:

In this scenario, the robot will repeat the orange trajectory ten times for each run. So the total running distance is around $10 \times 128m = 1280m$. The locations where feature matches between the map and the running VIO occur are marked in Fig. 12 (a) by black asterisks (20 locations for each loop). During the ten loops of each run, the feature matching only occurs in the second to fourth loop and the ninth to tenth loop (100 locations).

[2]Here, we neglect the IMU bias parts of (20), (29) and (30) for simplicity. Besides, only one map keyframe and one map landmark are considered, such that ${}^{G}\hat{\mathbf{p}}_{F_j,t}$ in (29) and (30) becomes ${}^{G}\hat{\mathbf{p}}_{F,t}$, and ${}^{G}\hat{\mathbf{R}}_{KF_i,t}$ becomes ${}^{G}\hat{\mathbf{R}}_{KF,t}$

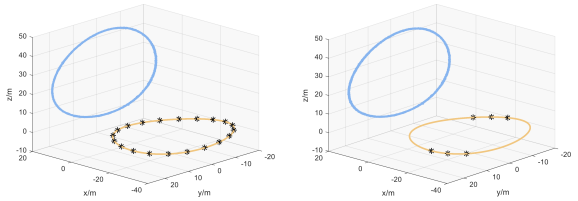

(a) (b)

Fig. 12. The trajectories used for simulation. The blue one is used to generate map information; The orange one is used to test algorithms; The black asterisks are the locations where feature matches between the test trajectory and the map trajectory occur. The difference between (a) and (b) is the number of locations where feature matching occur for each loop. (a) has 20 feature matching positions for each loop, while (b) has only six feature matching positions for each loop.

TABLE VI
RMSEs ($degree/m$) and NEESs of different algorithms on simulation data with an imperfect map in Scenario 1

Algorithms		local-pose	relative-trans	map-pose
Open-VINS	RMSE	0.233/0.144	—	—
	NEES	0.926/0.841	—	—
MSC-EKF	RMSE	1.109/0.472	0.777/0.256	0.612/0.369
	NEES	11.374/10.856	924.083/11.924	—
MSC-S-EKF	RMSE	0.821/0.373	0.863/0.167	0.206/0.094
	NEES	4.220/2.783	90.690/1.794	—
MSC-IKF	RMSE	0.203/0.211	0.628/0.167	0.612/0.381
	NEES	1.010/7.231	59.706/6.702	—
MSOC-S-IKF	RMSE	**0.168/0.110**	**0.180/0.113**	**0.160/0.084**
	NEES	0.879/0.985	1.491/1.203	—

— means there is no such variable to evaluate.

-Scenario 3:

In this scenario, the robot will repeat the orange trajectory ten times for each run. So the total running distance is around $10 \times 128m = 1280m$. The locations where feature matches between the map and the running VIO occur are marked in Fig. 12 (b) by black asterisks (6 locations for each loop). During the ten loops of each run, the feature matching always occurs for each loop (60 locations).

-Scenario 4:

In this scenario, the robot will repeat the orange trajectory ten times for each run. So the total running distance is around $10 \times 128m = 1280m$. The locations where feature matches between the map and the running VIO occur are marked in Fig. 12 (b) by black asterisks (6 locations for each loop). During the ten loops of each run, the feature matching only occurs in the second to fourth loop and the ninth to tenth loop (30 locations).

In the above four scenarios, the different algorithms (MSC-EKF, MSC-S-EKF, MSC-IKF, MSOC-S-IKF) are tested with *imperfect maps*. The results are given in Table VI $\sim$ Table IX.

-Discussion:

From the results, we can find that our proposed algorithm MSOC-S-IKF can always get the NEESs of local-pose and relative-trans around one, which means that MSOC-S-IKF can produce good consistent results. And thanks to the consistency of MSOC-S-IKF, its accuracy of the local-pose and the

TABLE VII
RMSEs ($degree/m$) AND NEESs OF DIFFERENT ALGORITHMS ON SIMULATION DATA WITH AN IMPERFECT MAP IN SCENARIO 2

Algorithms		local-pose	relative-trans	map-pose
Open-VINS	RMSE	0.233/0.144	—	—
	NEES	0.926/0.841	—	—
MSC-EKF	RMSE	1.163/0.531	1.799/0.854	0.708/0.429
	NEES	10.784/7.826	2078.349/66.448	—
MSC-S-EKF	RMSE	1.197/0.545	1.304/0.253	0.176/0.089
	NEES	10.994/6.949	229.683/4.059	—
MSC-IKF	RMSE	0.230/0.160	0.702/0.705	0.766/0.430
	NEES	0.925/2.356	70.365/59.687	—
MSOC-S-IKF	RMSE	**0.176/0.126**	**0.185/0.132**	**0.175/0.088**
	NEES	0.870/1.136	0.319/1.173	—

— means there is no such variable to evaluate.

TABLE VIII
RMSEs ($degree/m$) AND NEESs OF DIFFERENT ALGORITHMS ON SIMULATION DATA WITH AN IMPERFECT MAP IN SCENARIO 3

Algorithms		local-pose	relative-trans	map-pose
Open-VINS	RMSE	0.233/0.144	—	—
	NEES	0.926/0.841	—	—
MSC-EKF	RMSE	1.156/0.576	1.072/0.402	1.162/0.449
	NEES	10.745/11.561	198.157/17.533	—
MSC-S-EKF	RMSE	1.192/0.552	1.162/0.216	0.244/0.121
	NEES	11.091/7.010	162.431/2.415	—
MSC-IKF	RMSE	0.225/0.182	1.219/0.531	1.154/0.449
	NEES	0.951/4.549	114.974/39.608	—
MSOC-S-IKF	RMSE	**0.194/0.119**	**0.265/0.170**	**0.217/0.112**
	NEES	0.899/1.019	0.345/1.041	—

— means there is no such variable to evaluate.

relative-trans are the best among the compared algorithms.

Moreover, by comparing the results of MSOC-S-IKF from Table VI and Table VII or from Table VIII and Table IX, we can conclude that the delayed initialization of ${}^{L}\mathbf{T}_{G}$ and the long-time absence of map information will not harm the system consistency, but the accuracy of the results slightly decreases because of the less available map information. Also, in Scenario 4, because only a little map information is available, the accuracy of the results is the lowest (cf. Table IX). However, the consistency of our proposed algorithm is still good with a small amount of map information.

From the above tables, readers may find that the inconsistent algorithms (MSC-EKF, MSC-S-EKF) can sometimes have good or even competitive results for the map-pose, but the results for the local-pose and the relative-trans are poor. This is because 1) the map-based observation function provides a constraint for the map-pose; 2) These two algorithms fail to maintain the correct observability properties of the system (as mentioned in **Theorem 4** and **Theorem 7** of the manuscript).

Another interesting phenomenon is that when comparing the results of NEES of Scenario 1 and 2, or Scenario 3 and 4, we can find that for inconsistent algorithms (MSC-EKF, MSC-S-EKF, MSC-IKF), the values of NEES increase when there is a long absence of map information. This can be explained in terms of the SLAM problem: the *augmented variable* can be regarded as a 6 DoF SLAM feature maintained in the state. When the system requires the map information again after a large gap, this is equivalent to the feature *augmented variable* being observed again after a long interval, similar to a loop-closure occurs. For an inconsistent system, i.e., the covariance of the state is not properly propagated, the incorrect covariance will result in the incorrect observation fusion (loop-closure) and thus deteriorate the consistency of the system [3], [4].

TABLE IX
RMSEs ($degree/m$) AND NEESs OF DIFFERENT ALGORITHMS ON SIMULATION DATA WITH AN IMPERFECT MAP IN SCENARIO 4

Algorithms		local-pose	relative-trans	map-pose
Open-VINS	RMSE	0.233/0.144	—	—
	NEES	0.926/0.841	—	—
MSC-EKF	RMSE	1.116/0.504	2.155/1.090	1.299/0.460
	NEES	9.851/6.731	1009.517/108.099	—
MSC-S-EKF	RMSE	1.133/0.523	1.168/0.214	0.255/**0.148**
	NEES	9.713/6.139	75.895/1.510	—
MSC-IKF	RMSE	0.224/0.154	1.292/0.971	1.343/0.474
	NEES	0.908/1.789	149.274/102.462	—
MSOC-S-IKF	RMSE	**0.194/0.129**	**0.278/0.185**	**0.231**/0.149
	NEES	0.888/1.072	0.453/0.687	—

— means there is no such variable to evaluate.

APPENDIX H
NUMERICAL SIMULATION RESULTS ABOUT THE INITIALIZATION OF THE AUGMENTED VARIABLE

When we initialize the *augmented variable*, the initial value and the covariance of the *augmented variable* can be analytically derived as illustrated in Sec. VII-C of the main paper. However, in practice, the performance of the proposed algorithm is insensitive to the conservative covariance of the initial *augmented variable*. This is because the initial value of the *augmented variable* is accurate and therefore the corresponding linearization point of the EKF is accurate such that the EKF can be approximately regarded as the KF, which is not sensitive to the initial covariance [2]. For an extreme situation, as is shown in [1], we can assume the initialized *augmented variable* ${}^{L}\hat{\mathbf{T}}_{G_t}$ has an infinite covariance matrix.

This section we perform some numerical simulations to demonstrate the effect of the initial covariance of ${}^{L}\hat{\mathbf{T}}_{G_t}$.

-Numerical simulations:

The simulation setting is identical to Scenario 2 given in Appendix G, which is also identical to Sec. VIII-A of the main paper, except that the initial covariance of the transformation between the frame L and the frame G is different. Specifically, the initial covariance of ${}^{L}\hat{\mathbf{T}}_{G_t}$ changes from infinite to zero while the analytically derived initial covariance is used as a baseline. For the case that the initial covariance of ${}^{L}\hat{\mathbf{T}}_{G_t}$ is infinite, we utilize the updating step derived in [1]. The following table gives the RMSEs and NEESs of local-pose (pose in the local frame L), relative-trans (transformation between the frame L and the frame G), and map-pose (pose in the map frame G) generated by our proposed algorithm MSOC-S-IKF. All the results are taken from the average of 5 times Monte Carlo simulations.

In Table X, the units of the given initial covariance of ${}^{L}\mathbf{T}_{G}$ are m^2 for the translation part and rad^2 for the rotation part. The actual average initial error of ${}^{L}\mathbf{T}_{G}$ is $\begin{bmatrix}0.007 & 0.0125 & 0.011\end{bmatrix}^{\top}$ rad for the rotation part and $\begin{bmatrix}0.038 & 0.238 & 0.190\end{bmatrix}^{\top}$ m for the translation part. From Table X, we can find with the variant of initial covariance($1e^{-2}\mathbf{I}_6 \sim 1e^{4}\mathbf{I}_6$), the accuracy of local-pose, relative-trans, and map-pose changes little. However, when the initial covariance is extremely large ($\infty\mathbf{I}_6$) or extremely small ($1e^{-3}\mathbf{I}_6$, $1e^{-4}\mathbf{I}_6$, $0\mathbf{I}_6$), the NEESs of local-pose and/or relative-trans become large, which means the estimated value is inconsistent. Therefore, apart from deriving the covariance

TABLE X
RMSEs ($degree/m$) AND NEESs OF MSOC-S-IKF ON SIMULATION DATA WITH A IMPERFECT MAP

Initial Covariance of ${}^{L}\mathbf{T}_{G}$		local-pose	relative-trans	map-pose
$\infty\mathbf{I}_6$	RMSE	0.205/0.124	0.407/0.167	0.309/0.121
	NEES	0.874/0.959	10.089/3.087	—
$1e^4\mathbf{I}_6$	RMSE	0.175/0.120	0.175/0.123	0.186/0.090
	NEES	0.870/0.962	0.431/1.025	—
$1e^3\mathbf{I}_6$	RMSE	0.176/0.118	0.169/0.118	0.178/0.086
	NEES	0.870/0.935	0.365/0.936	—
$1e^2\mathbf{I}_6$	RMSE	0.176/0.118	0.169/0.117	0.178/0.086
	NEES	0.869/0.935	0.362/0.934	—
$50\mathbf{I}_6$	RMSE	0.176/0.118	0.169/0.117	0.178/0.086
	NEES	0.870/0.935	0.362/0.934	—
$20\mathbf{I}_6$	RMSE	0.176/0.118	0.169/0.117	0.178/0.086
	NEES	0.870/0.935	0.362/0.933	—
$10\mathbf{I}_6$	RMSE	0.176/0.118	0.169/0.117	0.178/0.086
	NEES	0.869/0.935	0.361/0.933	—
$1\mathbf{I}_6$	RMSE	0.173/0.118	0.163/0.116	0.175/0.085
	NEES	0.869/0.933	0.361/0.937	—
$1e^{-1}\mathbf{I}_6$	RMSE	0.163/0.117	0.146/0.108	0.172/0.082
	NEES	0.868/0.909	0.361/0.924	—
$1e^{-2}\mathbf{I}_6$	RMSE	0.127/0.110	0.138/0.124	0.177/0.081
	NEES	0.865/1.004	0.374/1.636	—
$1e^{-3}\mathbf{I}_6$	RMSE	0.288/0.166	0.369/0.279	0.189/0.085
	NEES	0.877/4.531	0.955/23.062	—
$1e^{-4}\mathbf{I}_6$	RMSE	0.470/0.228	0.592/0.356	0.190/0.085
	NEES	1.106/8.916	1.951/139.708	—
$0\mathbf{I}_6$	RMSE	0.498/0.267	1.023/0.378	0.827/0.215
	NEES	312.969/12.394	—	—
analytically derived	RMSE	0.191/0.124	0.175/0.112	0.169/0.082
	NEES	0.870/0.931	0.360/0.933	—

— means there is no such v ariable to evaluate.

analytically, giving a big value to the initial covariance of ${}^{L}\mathbf{T}_{G}$ is also a simple and safe strategy in practice.

REFERENCES

[1] R. C. DuToit, J. A. Hesch, E. D. Nerurkar and S. I. Roumeliotis, "Consistent map-based 3D localization on mobile devices," *2017 IEEE International Conference on Robotics and Automation (ICRA)*, Singapore, 2017, pp. 6253-6260, doi: 10.1109/ICRA.2017.7989741.

[2] X. Liu and A. Goldsmith, "Kalman filtering with partial observation losses," 2004 43rd IEEE Conference on Decision and Control (CDC) (IEEE Cat. No.04CH37601), 2004, pp. 4180-4186 Vol.4, doi: 10.1109/CDC.2004.1429408.

[3] S. J. Julier and J. K. Uhlmann, "A counter example to the theory of simultaneous localization and map building," Proceedings 2001 ICRA. IEEE International Conference on Robotics and Automation (Cat. No.01CH37164), 2001, pp. 4238-4243 vol.4, doi: 10.1109/ROBOT.2001.933280.

[4] J.A. Castellanos, J. Neira, and J.D. Tardos, "Limits to the consistency of EKF-based SLAM," In IFAC Symposium on Intelligent Autonomous Vehicles, 2004, pp. 716-721 vol.37, doi: 10.1016/S1474-6670(17)32063-3.